Drug Delivery

DOI: 10.1002/ange.201008053

Self-Assembly of a Bifunctional DNA Carrier for Drug Delivery**

Kelong Wang, Mingxu You, Yan Chen, Da Han, Zhi Zhu, Jin Huang, Kathryn Williams, Chaoyong James Yang, and Weihong Tan**

Herein, we propose a simple method for combining two functional DNA groups, such that one group is capable of recognizing the target cell, while a complementary group acts as a drug delivery carrier. This novel G-quadruplex–aptamer–drug platform takes advantage of the target-recognition function of a DNA aptamer and the drug-loading ability of a G-quadruplex.

The design and engineering are based on DNA self-assembly. DNA has been widely used as a building block in the design of self-assembled nanostructures because of its well-defined geometry and highly predictable and programmable interactions.[1–12] DNA can form a self-assembled pattern, either by itself[1,2,6,9] or in conjugation with other units, such as nanoparticles or carbon nanotubes.[3,11,13] Watson–Crick base-pairing is one internal driver of DNA self-assembly,[4] as Seeman's group has reported;[14–17] the formation of G-quadruplexes is yet another mode of self-assembly. Briefly, in a guanine-rich region of DNA, three or four guanine bases associate into a cyclic Hoogsten hydrogen-bonding arrangement, and the stack of G-quartets forms G-quadruplexes.[18,19] Compared to Watson–Crick base pairing, each guanine base makes two hydrogen bonds with its neighbors using different hydrogen-bonding positions. Stabilization of the G-quadruplex structure is achieved by such cations as K^+ and Na^+. More important to the present report, the photosensitizer 5,10,15,20-tetrakis-(1-methyl-4-pyridyl)-21*H*,23*H*-porphine (TMPyP4) tends to intercalate into G-quadruplex structures,[19–22] and, as such, it can be delivered to a target cell by a high-affinity aptamer. When activated by light of a specific wavelength, the photosensitizer transfers the light energy to molecular oxygen to generate reactive oxygen species (ROS), which mediate cellular toxicity.[23] Shieh et al. reported that aptamer As1411, which tends to form an intramolecular G-quadruplex, was able to selectively deliver TMPyP4 into MCF7 breast cancer cells. The As1411–TMPyP4 complex was resistant to degradation and digestion by the enzyme DNase I. Furthermore, As1411–TMPyP4 achieved higher target cell accumulation and cytotoxicity to MCF7 cells than TMPyP4 itself.[24]

Tan and co-workers have developed a DNA self-assembly strategy to form hydrogels for detection and controlled release.[25,26] Specifically, aptamers covalently linked with doxorubicin[27] and photosensitizer Ce6[28] were designed to achieve selective drug delivery. Herein, we report another novel self-assembly strategy, which combines the target-recognition function of a DNA aptamer and the drug-loading ability of a G-quadruplex. Both intermolecular G-quadruplex formation and drug loading are characterized, and the application of this bifunctional unit is demonstrated by selective delivery of a photosensitizer to cancer cells. Because of the selective G-quadruplex–aptamer delivery, the photosensitizer generated high toxicity to target cells and low toxicity to reference cells upon irradiation with white light. This scheme (Figure 1) may serve as a universal method for joining two functional groups by DNA self-assembly. Furthermore, it brings the promise of aptamer-based therapeutics closer to fruition.

Aptamers were first modified by guanine-rich segments capable of forming intermolecular G-quadruplexes after annealing in an appropriate buffer. The sequences were designed based on two single-stranded DNA (ssDNA) aptamers, Sgc8 and TD05 (see the Experimental Section for sequences). Sgc8 was selected for binding with CCRF-CEM cells (CEM), a human precursor T-cell acute lymphoblastic leukemia (T-ALL) cell line, and TD08 was selected for recognizing B-cell Burkitt's lymphoma cell line (Ramos cells).[29,30] Sgc8 modified with DNA segment T-4G-4T-4G-4T was demonstrated to form a G-quadruplex–aptamer module in buffer 1 (see the Supporting Information). We named this module G-quadruplex–Sgc8.

[*] Dr. K. Wang, M. You, Dr. Y. Chen, D. Han, Z. Zhu, J. Huang, Dr. K. Williams, Prof. Dr. W. Tan
Center For Research at Bio/nano Interface, Department of Chemistry and Department of Physiology and Functional Genomics, Shands Cancer Center, UF Genetics Institute and McKnight Brain Institute, University of Florida
Gainesville, FL 322611-7200 (USA)
Fax: (+1) 352-846-2410
E-mail: tan@chem.ufl.edu
Dr. Y. Chen, J. Huang, Prof. Dr. W. Tan
State Key Laboratory of Chemo/Biosensing and Chemometrics
College of Biology and College of Chemistry and Chemical Engineering
Hunan University, Changsha 410082 (P.R. China)
Dr. Y. Chen, Prof. C. J. Yang
State Key Laboratory of Physical Chemistry of Solid Surfaces
The Key Laboratory for Chemical Biology of Fujian Province
The Key Laboratory of Analytical Sciences
and Department of Chemical Biology, College of Chemistry and Chemical Engineering, Xiamen University
Xiamen 361005 (China)
Fax: (+86) 592-218-9959
E-mail: cyyang@xmu.edu.cn

[**] We thank the NIH for supporting this work. This work was also supported by the National Key Scientific Program of China (2011CB911000) and China National Grand Program on Key Infectious Disease (2009ZX10004-312). China National Scientific Foundation of China (20805038, 20620130427), and National Basic Research Program of China (2007CB935603, 2010CB732402).

Supporting information for this article is available on the WWW under http://dx.doi.org/10.1002/anie.201008053.

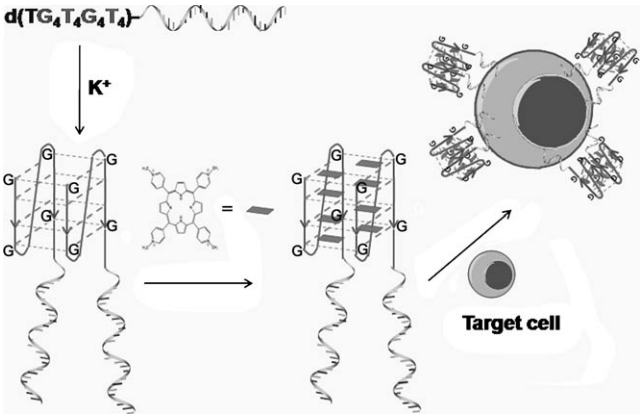

Figure 1. G-quadruplex–aptamer as a drug delivery carrier. The design utilizes the G-quadruplex as the drug carrier and the aptamer as the targeting molecule to deliver TMPyP4, which is known to bind and stabilize different types of quadruplexes. The helical strand represents the aptamer.

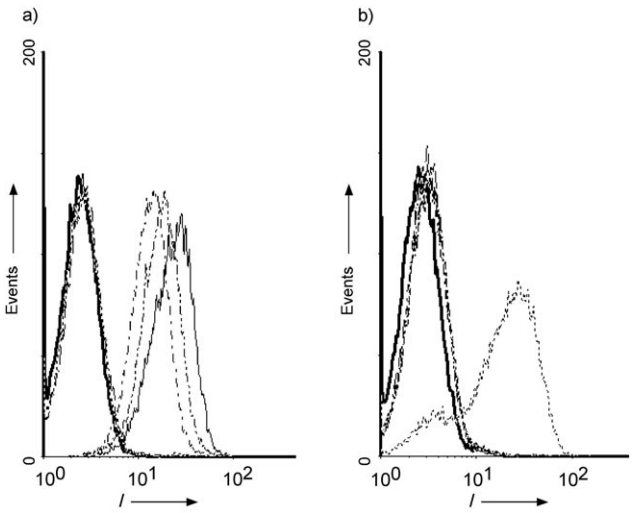

Figure 2. Binding of modified aptamer with a) CEM and b) Ramos cells. Different line styles represent different treatments: no treatment (bold solid), streptavidin–PE (dashed), G-quadruplex–Td05 (dotted), G-quadruplex–Sgc8 (dash-dot), 8G–Sgc8 (dash-double dot), and Sgc8 (solid). PE = Phycoerythin.

The formation of the G-quadruplex was tested by polyacrylamide gel electrophoresis (PAGE) and by circular dichroism (CD) spectroscopy. (Figures S1 and S3 in the Supporting Information) The binding of TMPyP4 with G-quadruplex–Sgc8 was tested by UV/Vis spectroscopy (Figure S4 in the Supporting Information). A Job's plot was then used to ascertain the number of TMPyP4 molecules bound per G-quadruplex (Figure S5 in the Supporting Information). A series of solutions containing different molar fractions of TMPyP4 and G-quadruplex–Sgc8 were prepared, with the total molar amount of reactants held constant. The absorbances of the mixtures at 422 and 438 nm were recorded (Figure S4 in the Supporting Information), and the absorbance difference was plotted versus the molar fraction of TMPyP4. The intersection of the two fitting lines showed that the molar fraction of TMPyP4 in the complex is 0.858, corresponding to a binding ratio of TMPyP4 to G-quadruplex–Sgc8 of 6:1. In addition to the high drug loading efficiency, the rate of drug leakage from the G-quadruplex carrier is slow; about $^1/_6$ of the intercalated TMPyP4 dissociated in 57 h (Figure S7 in the Supporting Information) at 37 °C. The slow leakage allows sufficient time for the carrier–drug complex to target the cancer cells without losing drug and minimizes possible side effects. Please refer to the Supporting Information for the details of aptamer optimization and G-quadruplex characterization.

The binding of modified aptamer with cells was studied by flow cytometry. CEM and Ramos cells were treated with G-quadruplex–Sgc8, G-quadruplex–TD05, biotin-T-4G-4T-4G-4T-Sgc8 (8G–Sgc8), and Sgc8 in H_2O and tested by flow cytometry. Figure 2 shows the fluorescence intensity changes, which correspond to the binding capacity of aptamer with cells. A larger fluorescence intensity shift corresponds to stronger binding of aptamers to the cells.

For the CEM cells (Figure 2a), the unmodified Sgc8 sequence showed the strongest binding, followed by 8G–Sgc8 in H_2O and G-quadruplex–Sgc8. The treatment of cells with G-quadruplex–Sgc8 showed a lower fluorescence intensity than the treatment with the aptamer without annealing. This lower intensity occurred either because the binding capacity between CEM cells and aptamer was slightly affected by the modification of the Sgc8 sequence or because the binding between biotin and streptavidin was hindered after formation of the intermolecular G-quadruplex. Treatment of CEM cells with G-quadruplex–TD05 did not generate a fluorescence peak shift, indicating that, as anticipated, G-quadruplex–TD05 did not bind to CEM. The binding of Ramos cells only with G-quadruplex–TD05 is shown in Figure 2b. This finding showed the selectivity of aptamers after modification. The biotin-T-4G-4T-4G-4T-Sgc8 sequence in both G-quadruplex formation and natural formation binds with CEM cells but not with Ramos cells. After modification of the aptamer with a segment of G-rich DNA and annealing, the binding selectivity was maintained, even though the binding capacity was slightly affected.

After the selectivity of the G-quadruplex–aptamer module was confirmed, the delivery of TMPyP4 by G-quadruplex–TMPyP4 and by TMPyP4 itself were compared in relation to their cytotoxicity to both CEM and Ramos cells. The cell toxicity tests were performed by measuring the cell viability by MTS assay (see the Experimental Section for details) after treatment by G-quadruplex–TMPyP4 or by TMPyP4 alone and irradiation. A DNA sequence complementary to the Sgc8 aptamer (denoted cDNA) was used as an antidote to control the delivery of TMPyP4. The results of cytotoxicity tests are summarized in Figure 3. In this bar chart, G-quadruplex represents annealed biotin-T-4G-4T-4G-4T-Sgc8 (G-quadruplex–Sgc8), and G-quadruplex–TMPyP4 represents the complex of TMPyP4 and G-quadruplex–Sgc8.

The results showed that without carrier, TMPyP4 generated a low cytotoxicity to both target cells and reference cells. With G-quadruplex–aptamer as the carrier module, the toxicity of TMPyP4 to the target cells doubled, but the reference cells were only slightly affected. With free TMPyP4 treatment, the relative viability of both CEM and Ramos cells

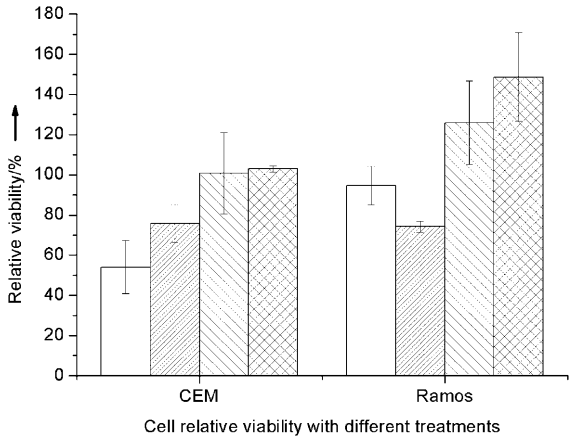

Figure 3. Cell relative viability with different treatments represented by four columns from left to right: G-quadruplex–TMPyP4, TMPyP4, G-quadruplex–TMPyP4 plus cDNA, G-quadruplex. The TMPyP4 concentration and irradiation time were optimized (data not shown): TMPyP4 100 nM, irradiation time 10 min at a light intensity of 0.28 $mW cm^{-2}$. The cells irradiated by the same lamp without drug treatment were considered to have 100% viability. The error bar is the standard deviation of nine replicates.

decreased to about 75%. When treated with G-quadruplex–TMPyP4, CEM cells showed an even lower viability (54%), thus indicating that treatment with G-quadruplex–TMPyP4 killed 21% more CEM cells than TMPyP4. On the contrary, the viability of Ramos cells was only slightly affected by the treatment with G-quadruplex–TMPyP4 (about 95%). The 20% increase of viability compared with the treatment with TMPyP4 showed the lower toxicity of G-quadruplex–TMPyP4 in Ramos cells. When the cDNA of Sgc8 aptamer was added to G-quadruplex–TMPyP4, the viability was about 100% for CEM cells. This result showed that the cDNA can be used as an antidote during treatment. The addition of G-quadruplex without TMPyP4 increased the viability of Ramos cells by about 50%, possibly because addition of G-quadruplex–Sgc8 triggers the proliferation of Ramos or because the addition of G-rich DNA segments provides more building blocks for cell proliferation. This result demonstrated that the delivery of TMPyP4 by G-quadruplex–TMPyP4 generated higher phototoxicity to CEM cells with very little toxicity to Ramos cells.

Comparing with the results of Shieh et al., the current design has the advantages of low drug concentration, less incubation time, and lower irradiation energy. Shieh et al. reported a TMPyP4 delivery platform by AS1411 aptamer to decrease the target cell viability by around 50% with 1 μM TMPyP4, 2 h incubation for drug uptake, and 1278 $mJ cm^{-2}$ irradiation energy (180 s at 7.1 $mW cm^{-2}$).[24] Even though different cell lines were studied, our G-quadruplex–aptamer module achieved similar results with 10 times less TMPyP4, 12 times shorter incubation time, and 7.6 times lower irradiation intensity (10 min at 0.28 $mW cm^{-2}$). The lower drug concentration and irradiation intensity will significantly decrease side effects of photodynamic treatment.

We expect that this technique may be applied in photodynamic treatment of cancers such as leukemia and lymphoma. Besides that, this method may be applied to deliver other reagents, such as fluorescence imaging reagents, as long as the reagents can form complexes with the G-quadruplex. However, the limited kinds of aptamers currently available hinder the wide application of this method. This is a more general demonstration of phototherapy with aptamers. The T cell leukemia cell line was used for convenience, because the aptamer Sgc8 targeting it has been selected previously. Also, the interaction of the carrier–drug complex with target cells needs to be studied, including the following questions: 1) Where is G-quadruplex–aptamer mainly localized after incubation with cells? Does it bind on the cell membrane and stay there, or is it internalized into the cell? 2) If it is internalized, at what organelle will it be enriched? 3) How long does the G-quadruplex circulate the in the cell or the body? By addressing these questions, an optimized photodynamic treatment based on the G-quadruplex–aptamer module could be designed to achieve maximum benefit and minimum side effects.

In conclusion, we proposed herein a simple method for combining two functional DNA groups. In this way, increased toxicity to the target cells was achieved during photodynamic therapy, while the cytotoxicity of the photosensitizer to the nontarget cells was minimized. DNA complementary to the aptamer can be utilized as an antidote to control the delivery of photosensitizer. We anticipate that the G-quadruplex–aptamer–drug platform based on the intercalation of TMPyP4 within the G-quadruplex may be utilized to develop novel effective cancer chemotherapy methodologies. In the future, we plan to evaluate the internalization of the G-quadruplex–aptamer–drug complex in cancer cells and then test the in vivo efficacy in animal models.

Experimental Section

Cell culture: CCRF-CEM (CCL-119, T-cell line, human acute lymphoblastic leukemia) and Ramos (CRL-1596, B-cell line, human Burkitt's lymphoma) cells were obtained from American Type Culture Collection. Cells were cultured in RPMI 1640 containing 10% fetal bovine serum (FBS, 10%), and penicillin–streptomycin (100 IU mL^{-1}) at 37°C in a humid atmosphere with 5% CO_2.

Aptamers: Aptamer and modified aptamer sequences with a 5′-disulfide group were synthesized on the ABI3400 DNA/RNA synthesizer (Applied Biosystems, Foster City, CA, USA). The completed sequences were then deprotected in AMA (ammonium hydroxide/40% aqueous methylamine 1:1) at 65°C for 20 min and further purified by reversed-phase HPLC (ProStar, Varian, Walnut Creek, CA, USA) on a C-18 column. The concentration of aptamer was determined with a Cary 100 Bio UV/Visible spectrophotometer (Varian, Inc.).

Sgc8 sequence: A TCT AAC TGC TGC GCC GCC GGG AAA ATA CTG TAC GGT TAG A

cDNA of Sgc8: ACG ACG CGG CGG CCC TTT TAT GAC ATG CCA ATC T

TD05 sequence: AAC ACC GTG GAG GAT AGT TCG GTG GCT GTT CAG GGT CTC CTC CGG TG

Buffer and annealing: Buffer 1: 200 mM KCl, 28 mM Tris-HCl, 4 mM $MgCl_2$, pH 8. Buffer 2: 100 mM KCl, 10 mM Tris-HCl, 1 mM Na_2EDTA, pH 7.5. Tris = Tris(hydroxymethyl) aminomethane, EDTA = ethylenediaminetetraacetic acid. G-modified aptamer (40 μM) was annealed from 93 to 22°C overnight and stored at 4°C.

Circular dichroism tests: Annealed aptamer 10 μM in buffer 1, annealed aptamer in TMPyP4, and TMPyP4 only were tested using an

AVIV Model 400 circular dichroism spectrophotometer (Aviv Biomedical, Inc., NJ, USA) from 200 to 350 nm.

UV absorption titration: The titration was performed with a Cary 100 Bio UV/Visible spectrophotometer (Varian, Inc.). The TMPyP4 was diluted to 10 μM. Different ratios of annealed G-quadruplex–Sgc8 in buffer 1 versus TMPyP4 were tested. The total molar concentration of the aptamer and TMPyP4 was held constant, but their fractions were varied to obtain the Job's Plot.

Steady-state fluorescence: The steady-state fluorescence measurements were recorded in a 1 cm × 0.2 cm quartz cell with a band pass of 5 nm for both excitation and emission by a Fluorolog-Tau-3 spectrofluorometer (Jobin Yvon, Edison, NJ). Emission spectra at 420 nm excitation wavelength were tested after incubation at 4 °C for 30 min.

Transmission electron microscopy (TEM): G-quadruplex–Sgc8–TMPyP4 complex was dropped onto carbon-coated 200 mesh copper grids. Grids were placed on delicate-task-wipers to absorb excess liquid and then dried in a desiccator overnight. The dried copper grid with the complex was examined under a Hitachi H-7000 transmission electron microscope (Hitachi, JAPAN).

Leakage of TMPyP4: To determine the leakage profile of TMPyP4 from the G-quadruplex–aptamer, the free TMPyP4 drug and the G-quadruplex–Sgc8–TMPyP4 complex in 200 μL buffer 1 were placed in Amicon Ultra-0.5 centrifugal filter devices with a cutoff of 30 kDa molecules. The centrifugal filter devices were soaked in 1.1 mL buffer 1 in the filtrate collection tubes and incubated at 37 °C. After 3, 7.25, and 21.25 h, 120 μL buffer was removed to measure the TMPyP4 fluorescence using a FluoroMax-4 Spectrofluorometer (Jobin Yvon, Edison, NJ; excitation wavelength 420 nm; emission wavelength 660 nm) and then poured back into the filtrate collection tubes. After incubating 57 h at 37 °C, the centrifugal devices were spun for 15 min at 14000 rpm, and the fluorescence intensity of the filtrate was tested.

Binding of G-quadruplex–aptamer with cells: The CEM and Ramos cells were washed with washing buffer and resuspended in binding buffer. Cells were split between six tubes for testing: cells only, cells plus streptavidin–PE, and cells with four different aptamers individually plus streptavidin–PE. Cells were incubated on ice for 10 min for aptamer binding and 20 min for dye binding. The cells were washed with 1.0 mL washing buffer and tested by a FACScan cytometer (Becton Dickinson Immunocytometry Systems, San Jose, CA, USA) by counting 20000 events.

Cytotoxicity test: Cell toxicity was tested by measuring the cell viability by MTS assay (CellTiter 96 AQ_{ueous} Non-Radioactive Cell Proliferation Assay, Promega Corporation, Madison, Wisconsin, USA) after treatment with G-quadruplex–TMPyP4 or TMPyP4 alone and irradiation. Cells irradiated by the same lamp without drug treatment were considered to be 100% viable. The TMPyP4 concentration and irradiation time were optimized at 100 nM and 10 min at 0.28 mW cm^{-2}. MTS involves colorimetric assays for measuring the activity of enzymes that reduce MTS (3-(4,5-dimethylthiazol-2-yl)-5-(3-carboxymethoxyphenyl)-2-(4-sulfophenyl)-2H-tetrazolium) or close dyes (XTT (sodium 3-[1-(phenylaminocarbonyl)-3,4-tetrazolium]-bis(4-methoxy-6-nitro) benzene sulfonic acid hydrate), MTT (3-(4,5-dimethylthiazol-2-yl)-2,5-diphenyltetrazoliumbromide)) to formazan. In brief, CEM and Ramos cells were cultured at a density of 5×10^4 cells per well (in 100 μL fresh medium) in flat-bottomed 96-well plates. After 24 h, MTS assay reagent was added to each well according to the manufacturer's instructions. After 4 h in culture, the cell viability was determined by measuring the absorbance at 490 nm using a 550 BioRad plate-reader (Bio-Rad, Hertfordshire, UK).

Received: December 20, 2010
Revised: February 25, 2011
Published online: May 18, 2011

Keywords: aptamers · DNA · drug delivery · G-quadruplexes · self-assembly

[1] Y. He, Y. Tian, Y. Chen, A. E. Ribbe, C. Mao, *Chem. Commun.* **2007**, 165 – 167.
[2] P. W. K. Rothemund, *Nature* **2006**, *440*, 297 – 302.
[3] J. Sharma, R. Chhabra, Y. Liu, Y. Ke, H. Yan, *Angew. Chem.* **2006**, *118*, 744 – 749; *Angew. Chem. Int. Ed.* **2006**, *45*, 730 – 735.
[4] B. Samorì, G. Zuccheri, *Angew. Chem.* **2005**, *117*, 1190 – 1206; *Angew. Chem. Int. Ed.* **2005**, *44*, 1166 – 1181.
[5] C. Lin, Y. Liu, S. Rinker, H. Yan, *ChemPhysChem* **2006**, *7*, 1641 – 1647.
[6] Y. He, T. Ye, M. Su, C. Zhang, A. E. Ribbe, W. Jiang, C. Mao, *Nature* **2008**, *452*, 198 – 201.
[7] F. A. Aldaye, P. K. Lo, P. Karam, C. K. McLaughlin, G. Cosa, H. F. Sleiman, *Nat. Nanotechnol.* **2009**, *4*, 349 – 352.
[8] K. M. M. Carneiro, F. A. Aldaye, H. F. Sleiman, *J. Am. Chem. Soc.* **2010**, *132*, 679 – 685.
[9] S. M. Douglas, H. Dietz, T. Liedl, B. Hogberg, F. Graf, W. M. Shih, *Nature* **2009**, *459*, 414 – 418.
[10] P. K. Lo, P. Karam, F. A. Aldaye, C. K. McLaughlin, G. D. Hamblin, G. Cosa, H. F. Sleiman, *Nat. Chem.* **2010**, *2*, 319 – 328.
[11] S. Pal, J. Sharma, H. Yan, Y. Liu, *Chem. Commun.* **2009**, 6059 – 6061.
[12] F. Rakotondradany, A. Palmer, V. Toader, B. Chen, M. A. Whitehead, H. F. Sleiman, *Chem. Commun.* **2005**, 5441 – 5443.
[13] S. Lyonnais, C. L. Chung, L. Goux-Capes, C. Escude, O. Pietrement, S. Baconnais, E. Le Cam, J. P. Bourgoin, A. Filoramo, *Chem. Commun.* **2009**, 683 – 685.
[14] E. Winfree, F. Liu, L. A. Wenzler, N. C. Seeman, *Nature* **1998**, *394*, 539 – 544.
[15] N. C. Seeman, *Nature* **2003**, *421*, 427 – 431.
[16] C. Mao, T. H. LaBean, J. H. Relf, N. C. Seeman, *Nature* **2000**, *407*, 493 – 496.
[17] N. C. Seeman, *Annu. Rev. Biochem.* **2010**, *79*, 65 – 87.
[18] H. J. Lipps, D. Rhodes, *Trends Cell Biol.* **2009**, *19*, 414 – 422.
[19] J. T. Davis, *Angew. Chem.* **2004**, *116*, 684 – 716; *Angew. Chem. Int. Ed.* **2004**, *43*, 668 – 698.
[20] L. Martino, B. Pagano, I. Fotticchia, S. Neidle, C. Giancola, *J. Phys. Chem. B* **2009**, *113*, 14779 – 14786.
[21] A. N. Lane, J. B. Chaires, R. D. Gray, J. O. Trent, *Nucleic Acids Res.* **2008**, *36*, 5482 – 5515.
[22] H. Zhang, X. Wang, P. Wang, S. Pang, X. Ai, J. Zhang, *Sci. China Ser. B* **2008**, *51*, 452 – 456.
[23] D. E. J. G. J. Dolmans, D. Fukumura, R. K. Jain, *Nat. Rev. Cancer* **2003**, *3*, 380 – 387.
[24] Y.-A. Shieh, S.-J. Yang, M.-F. Wei, M.-J. Shieh, *Acs Nano* **2010**, *4*, 1433 – 1442.
[25] Z. Zhu, C. Wu, H. Liu, Y. Zou, X. Zhang, H. Kang, C. J. Yang, W. Tan, *Angew. Chem.* **2010**, *122*, 1070 – 1074; *Angew. Chem. Int. Ed.* **2010**, *49*, 1052 – 1056.
[26] H. Yang, H. Liu, H. Kang, W. Tan, *J. Am. Chem. Soc.* **2008**, *130*, 6320 – 6321.
[27] Y. F. Huang, D. Shangguan, H. Liu, J. A. Phillips, X. Zhang, Y. Chen, W. Tan, *ChemBioChem* **2009**, *10*, 862 – 868.
[28] P. Mallikaratchy, Z. W. Tang, W. H. Tan, *ChemMedChem* **2008**, *3*, 425 – 428.
[29] D. Shangguan, Z. C. Cao, Y. Li, W. Tan, *Clin. Chem.* **2007**, *53*, 1153 – 1155.
[30] Z. Tang, D. Shangguan, K. Wang, H. Shi, K. Sefah, P. Mallikratchy, H. W. Chen, Y. Li, W. Tan, *Anal. Chem.* **2007**, *79*, 4900 – 4907.

